Fluctuating charge order in the cuprates: Spatial anisotropy and feedback from superconductivity

Yuxuan Wang, Debanjan Chowdhury, and Andrey V. Chubukov

Phys. Rev. B **92**, 161103 — Published 7 October 2015

DOI: 10.1103/PhysRevB.92.161103

Fluctuating charge order in the cuprates: spatial anisotropy and feedback from superconductivity

Yuxuan Wang,[1,2] Debanjan Chowdhury,[3] and Andrey V. Chubukov[4]

[1] *Department of Physics, University of Wisconsin, Madison, WI 53706, USA*
[2] *Department of Physics and Institute for Condensed Matter Theory, University of Illinois at Urbana-Champaign, 1110 West Green Street, Urbana, Illinois, 61801, USA*
[3] *Department of Physics, Harvard University, Cambridge, MA 02138, USA*
[4] *William I. Fine Theoretical Physics Institute, and School of Physics and Astronomy, University of Minnesota, Minneapolis, MN 55455, USA*

We analyze the form of static charge susceptibility $\chi(q)$ in underdoped cuprates near axial momenta $(Q,0)$ and $(0,Q)$ at which short-range static charge order has been observed. We show that the momentum dependence of $\chi(q)$ is anisotropic, and the correlation length in the longitudinal direction is larger than in the transverse direction. We show that correlation lengths in both directions decrease once the system evolves into a superconductor, as a result of the competition between superconductivity and charge order. These results are in agreement with resonant x-ray scattering data [R. Comin et al., Science **347**, 1335 (2015)]. We also argue that density and current components of the charge order parameter are affected differently by superconductivity – the charge-density component is reduced less than the current component and hence extends deeper into the superconducting state. This gives rise to two distinct charge order transitions at zero temperature.

Introduction.- Understanding charge order (CO) in high-T_c cuprates and its interplay with superconductivity is essential for the understanding of the complex phase diagram of these materials. An incommensurate charge order, accompanied by spin-order, was originally discovered in La-based cuprates[1,2], but recently was also found to occur in Y- Bi-, and Hg- based materials[3–9], without an accompanying spin-order. A true long-range charge order has so far been observed only in a finite magnetic field[9], but a short-range static order (probably pinned by impurities) has been detected already in zero field. The CO has an axial momentum $\mathbf{Q} = Q_y = (0,Q)$ or $Q_x = (Q,0)$ with $Q \sim (0.2-0.3)\times 2\pi$, and can potentially be uni-axial (stripe)[10,11], with only Q_x or Q_y within a given domain, or bi-axial (checkerboard) with Q_x and Q_y present in every domain. Recent STM and x-ray experiments[12–14] point towards the uni-axial order, at least at small values of the doping. The CO is often termed as charge-density-wave (CDW) to emphasize that it develops with finite incommensurate momenta, although its on-site component is subleading to its bond component because the measured form-factor for CO has predominantly a d-wave form[8].

The origin of the CO is still a subject of intense debates[15–27]. Within one scenario, the charge order is induced by soft antiferromagnetic fluctuations[15–18]. This fits into the generic scenario that antiferromagnetism is the primary order parameter (i.e., the one whose fluctuations develop already at "high" energies, comparable to the bandwidth), while CDW, its cousin pair-density-wave (PDW), and uniform d-wave superconductivity all develop as secondary orders induced by soft, low-energy magnetic fluctuations before the system becomes magnetically ordered. In another scenario, charge order is induced by lattice vibrations[28]; in this case lattice and electronic degrees of freedom should be taken into account on an equal footing. And in yet another scenario, CO emerges in the process of the system transformation from a conventional metal to a Mott insulator[29]. If charge order reflects the crossover towards Mott physics, then the tendency towards localization of electronic states cannot be neglected even above optimal doping.

One way to distinguish between these scenarios is to use the existing experimental data, particularly the ones for which the data analysis does not involve fitting parameters. Recent x-ray scattering data in underdoped YBCO, reported in Ref. 13, can be used for this purpose. The data shows that the momentum structure of the static[30] charge susceptibility $\chi(\omega = 0, q)$ near Q_x and Q_y is anisotropic, and the longitudinal correlation length is larger than the transverse one, i.e. if $\chi(q)$ at $\mathbf{q} = \mathbf{Q} + \tilde{\mathbf{q}}$ is approximated by a Lorentzian $\chi^{-1}(q) \sim \xi^{-2} + A_\parallel^2 \tilde{q}_\parallel^2 + A_\perp^2 \tilde{q}_\perp^2$, then $A_\parallel > A_\perp$. In this paper, we verify whether this condition is reproduced within the two itinerant-electronic scenarios – the magnetic one and the phonon one. Exploring the Mott scenario is beyond the scope of this work.

Methods.- The charge susceptibility of itinerant electrons, $\chi(q)$, is generally related by a Random-phase-approximation-type (RPA) formula to the static particle-hole polarization bubble between low-energy fermions separated by approximately $\mathbf{Q}$ ("hot" fermions). We shall start with either the magnetic or the phonon scenario as our input assumptions. Our analysis departs from microscopic models, and is in this respect complementary to some earlier phenomenological analyses[31]. The difference between these two scenarios is that in the magnetic one the interaction is peaked at momentum $\mathbf{K} = (\pi,\pi)$ and connects fermions from two different hot regions. Specifically, magnetic interaction moves the center of mass momentum of a pair of hot fermions from $\mathbf{k}_0$ to $\mathbf{k}_\pi = \mathbf{k}_0 + \mathbf{K}$. Then, one needs to apply spin-fluctuation mediated scattering twice to move fermions back to the same hot region (see Fig. 1), and, as a con-

sequence, $\chi^{-1}(q) \propto 1 - V_{\rm sf}^2\ \Pi_{k_0}(\mathbf{q})\Pi_{k_\pi}(\mathbf{q})$, where $V_{\rm sf}$ represents the strength of the spin-fluctuation mediated scattering and $\Pi_{k_0}(\mathbf{q})$, $\Pi_{k_\pi}(\mathbf{q})$ are polarization operators made out of hot fermions with relative momentum $\mathbf{q}$ and center of mass momentum near $\mathbf{k}_0$ and $\mathbf{k}_\pi$, respectively (see Fig. 2a). In the phonon scenario, the interaction acts independently within each hot region, and $\chi^{-1}(q) \propto 1 - V_{\rm ph}[\Pi_{k_0}(\mathbf{q}) + \Pi_{k_\pi}(\mathbf{q})]$,where $V_{\rm ph}$ is the phonon-mediated interaction. In both cases, the momentum dependence of $\chi(q)$ is solely determined by the polarization bubbles and does not depend on the strength of the interaction $V_{\rm sf}$ or $V_{\rm ph}$.

The polarization bubbles $\Pi_{k_0}(\mathbf{q})$ and $\Pi_{k_\pi}(\mathbf{q})$ depend on the Fermi surface geometry in the vicinity of the hot spots and also on the choice of the upper cutoff in the momentum deviations from the hot spots. The presence of the cutoff, Λ, reflects the fact that the interaction in the charge channel can be approximated by a constant ($V_{\rm sf}$ or $V_{\rm ph}$) only in a finite range around a hot spot, outside of which it drops rapidly. In particular, within spin-fluctuation scenario, Λ depends on the distance to the magnetic QCP – it tends to a constant at the QCP and scales as inverse magnetic correlation length ξ_s^{-1}, when ξ_s drops below a certain value[27,32].

We report the analytical results for $\Pi_{k_0}(q)$ and $\Pi_{k_\pi}(q)$ using a hard cutoff (to be defined below). In the magnetic scenario, the longitudinal charge correlation length turns out to be larger than the transverse one, in agreement with the data[13]. For the phonon scenario, the result is the opposite – the transverse correlation length is larger. Taken at face value, the magnetic mechanism of CO better agrees with the experimental observation. We caution, however, that a more sophisticated analysis, which, e.g., includes the momentum dependence of the effective interaction, is needed to truly distinguish the two scenarios.

We also consider how charge susceptibility $\chi(q)$ gets modified once the system becomes superconducting. We find that the key effect of superconductivity is the reduction of $\Pi_{k_0}(\mathbf{Q})$ and $\Pi_{k_\pi}(\mathbf{Q})$ due to competition between CO and superconducting order parameters. As a result, both longitudinal and transverse CO correlation lengths get smaller in the superconducting state. A more subtle result is that this reduction is different for density and current components of CO. The two are symmetric and antisymmetric combinations of the incommensurate charge order parameters $\Delta_k^Q \equiv c^\dagger_{k+Q/2,\alpha}\delta_{\alpha\beta}c_{k-Q/2,\beta}$ with $k = \pm k_0$. The current component changes sign under time-reversal and once it develops along with the density component, the CO spontaneously breaks time-reversal symmetry[18,33]. In the normal state, density and current susceptibilities are equal [both are $\chi(q)$], as long as $\mathbf{k}_0$ and $-\mathbf{k}_0$ are well separated such that one can neglect bilinear coupling between $\Delta_{k_0}^Q$ and $\Delta_{-k_0}^Q$. In the superconducting state, $\chi^{-1}(\mathbf{Q})$ for the current component of CO gets shifted by $\Delta_{sc}^2/(T\Lambda v_F)$ due to negative feedback from long-range superconducting order, Δ_{sc}. For the density component of CO, such term cancels out and the shift is much smaller, of order $\Delta_{sc}^2/(\Lambda v_F)^2 \times \log(\Lambda/T)$. As a result, the density component of CO is much less affected by superconductivity and should persist deeper into the superconducting state. This is in agreement with the x-ray data, which found that the measured charge density fluctuations persist deep into the superconducting state[13], where they also likely get pinned by quenched disorder[34]. Meanwhile, at zero temperature, the CO emerging from pre-existing superconducting state should initially have no current component.

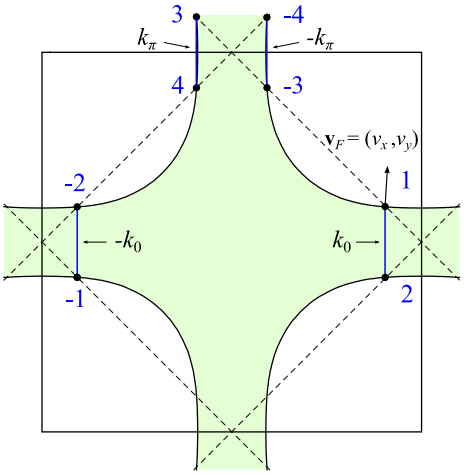

FIG. 1. The Fermi surface (black) with the occupied states shown in green. The location of the hot spots for CO (the points on the Fermi surface separated by $Q_y = (0, Q)$ or $Q_x = (Q, 0)$) are marked as $1, 2, -1, -2, ...$ with the corresponding directions of Fermi velocities, v_F. The notations $\pm k_0$ and $\pm k_\pi$ are for the center of mass momentum of charge order parameter $\Delta_k^Q = c^\dagger_{k+Q/2,\alpha}\delta_{\alpha\beta}c_{k-Q/2,\beta}$.

Polarization operators in the normal state.- For the computation of polarization operators we used the Fermi surface shown in Fig. 1. For definiteness we set $\mathbf{Q} = \mathbf{Q}_y = (0, Q)$. The results for $\mathbf{Q} = \mathbf{Q}_x$ are identical by a $\pi/2$ rotation. There are four "hot" regions in the Brillouin zone. For the two regions with $\mathbf{k}_0 = (\pi - Q/2, 0)$ and $-\mathbf{k}_0$, the Fermi velocity of the two fermions separated by $\mathbf{Q}$ are almost anti-parallel, while for the other two, with $\mathbf{k}_\pi = (-Q/2, \pi)$ and $-\mathbf{k}_\pi$, the velocities are nearly parallel. In the notations in Fig. 1, this implies $v_y \gg v_x$ ($v_y/v_x \approx 13.6$ in BSCCO, see Ref. 35).

We impose a hard cutoff by requiring that momentum of each fermion in the particle-hole bubble $\Pi_{k_0}(q)$ and $\Pi_{k_\pi}(q)$ differs from the corresponding hot spot by no more than Λ by amplitude. In the hot region with center of mass momentum of a pair near k_0 we define $\mathbf{k}_{1,2} = \mathbf{k}_0 \pm (\mathbf{Q}_y + \tilde{\mathbf{q}})/2 + \tilde{\mathbf{k}}$, and the condition reads $|\tilde{\mathbf{k}} \pm \tilde{\mathbf{q}}/2| < \Lambda$. The analogous condition holds in the hot region with center of mass momentum of a pair near k_π. We assume that Λ is small compared with inverse lattice spacing, in which case we can expand the dispersion of a hot fermion to linear order in deviation from a hot spot. Under these condition, we obtained analyt-

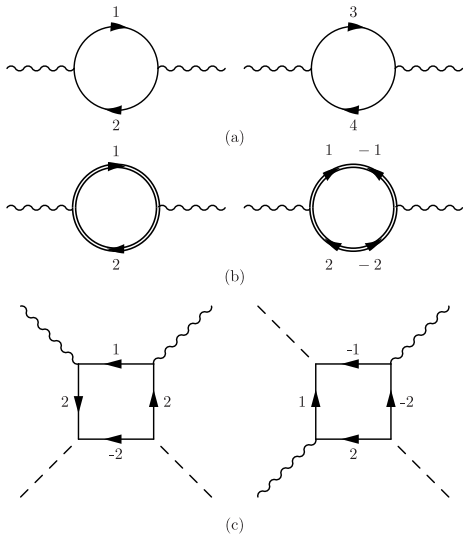

FIG. 2. The Feynman diagrams for (a) $\Pi_{k_0}(Q)$ and $\Pi_{k_\pi}(Q)$ in the normal state, and, (b) normal and anomalous contributions to $\Pi_{k_0}(Q)$ in the superconducting state. (c) Four-point diagrams contributing to β_{11} and β_{12} in the free-energy [Eq. (2)] in the normal state.

ical expressions for the polarization bubbles $\Pi_{k_0}(q)$ and $\Pi_{k_\pi}(q)$ to leading order in $\tilde{\mathbf{q}} = \mathbf{q} - \mathbf{Q}_y$. The calculation is lengthy but straightforward[36], and the result is

$$\Pi_{k_0}(\tilde{\mathbf{q}}) = Av_x \left(2\Lambda \log \tfrac{v+v_y}{v_x} - |\tilde{q}_y| \sin^{-1} \tfrac{v_y}{v} - |\tilde{q}_x| \log \tfrac{v}{v_x}\right),$$
$$\Pi_{k_\pi}(\tilde{\mathbf{q}}) = Av_y \left(2\Lambda \log \tfrac{v+v_x}{v_y} - |\tilde{q}_y| \sin^{-1} \tfrac{v_x}{v} - |\tilde{q}_x| \log \tfrac{v}{v_y}\right) \quad (1)$$

where $v = \sqrt{v_x^2 + v_y^2}$ and $A = 1/(\pi^2 v_x v_y)$. It is interesting to note that the singular terms proportional to $|\tilde{q}_{x,y}|$ are independent of the cutoff, Λ.

The case of the hard cutoff is somewhat special because the expansion of polarization bubbles in $\tilde{\mathbf{q}}$ is non-analytic and holds in powers of $|\tilde{q}_x|$ and $|\tilde{q}_y|$ rather than in $\tilde{q}_x^2$ and $\tilde{q}_y^2$. *We verified that the quadratic dependence emerges immediately once we soften the cutoff.* Still, even for the strictly hard cutoff one can analyze the anisotropy of the inverse charge susceptibility $\chi^{-1}(q)$ by comparing the prefactors for longitudinal ($|\tilde{q}_y|$) and transverse ($|\tilde{q}_x|$) momentum dependencies. By continuity, the anisotropy should survive upon softening of the cutoff.

To analyze the anisotropy, we use $v_y \gg v_x$ and expand Π_{k_0} and Π_{k_π} in small v_x/v_y limit[36]. In the magnetic scenario we find $\chi^{-1}(q) \propto C_0 + C_y|\tilde{q}_y| + C_x|\tilde{q}_x| + ...$, where $C_0 = 1/V_{\rm sf}^2 - 4A^2\Lambda^2 v_x^2 \log 2v_y/v_x$, $C_y = 2A^2\Lambda v_x^2(\log 2v_y/v_x + \pi/2), C_x = 2A^2\Lambda v_x^2 \log v_y/v_x$ and the ellipses denote higher order terms in $\tilde{q}_{x,y}$. We remind that $\mathbf{q} = \mathbf{Q}_y + \tilde{\mathbf{q}}$, hence $\tilde{q}_y$ is longitudinal component. Taking the ratio C_y/C_x we immediately see that $C_y/C_x = 1 + [(\pi/2 + \log 2)/\log(v_y/v_x)] > 1$, i.e., the effective correlation length $\xi_\parallel = C_y/C_0$ is larger than $\xi_\perp = C_x/C_0$. This is consistent with the data[13]. For $v_y/v_x \approx 13.6$, we obtained, without expanding, $\xi_\parallel/\xi_\perp = 1.87$, which is reasonably close to the experimental ratio of around 1.5. In the phonon scenario we obtain $\chi^{-1}(q) \propto \bar{C}_0 + \bar{C}_y|\tilde{q}_y| + \bar{C}_x|\tilde{q}_x| + ...$, where now, to logarithmic accuracy, $\bar{C}_y/\bar{C}_x = (\pi/2+1)/\log(v_y/v_x)$. Then $\bar{C}_y/\bar{C}_x$ is smaller than one, at least when v_y/v_x is large enough. For $v_y/v_x \approx 13.6$, we obtained, without expanding, $\xi_\parallel/\xi_\perp = 0.98$.

We also computed $\Pi_{k_0}(\tilde{\mathbf{q}})$ and $\Pi_{k_\pi}(\tilde{\mathbf{q}})$ numerically for a specific Lorentzian cutoff, which we imposed by inserting into the integrands for the bubbles an additional factor, $\Lambda^2/(\Lambda^2 + (\tilde{\mathbf{k}} + \tilde{\mathbf{q}}/2)^2) \times \Lambda^2/(\Lambda^2 + (\tilde{\mathbf{k}} - \tilde{\mathbf{q}}/2)^2)$, but not restricting integration over momentum. One can immediately make sure that in this case the expansion in $\tilde{q}$ holds in powers of $\tilde{q}^2$. We again find that in a magnetic scenario $\xi_\parallel/\xi_\perp > 1$. However this ratio is much larger. From this perspective, the hard cutoff gives better agreement with the data. We don't have analytic understanding why this is the case.

Superconducting state.- The polarization operators $\Pi_{k_0}(q)$ and $\Pi_{k_\pi}(q)$ in the superconducting state are obtained in a conventional way, by combining bubbles made out of normal and anomalous fermionic Green's functions (Fig. 2b). The full expressions are more involved and we did not obtain analytical formulas even for a hard cutoff. In general, both $\Pi_{k_0}(\mathbf{Q}_y)/\Pi_{k_\pi}(\mathbf{Q}_y)$ and the momentum-dependent terms in the polarization operators evolve with the superconducting gap Δ_{sc}. The effect, however, is stronger for $\chi(\mathbf{Q}_y)$ rather than for $\tilde{q}$-dependent terms because for $\chi(\mathbf{Q}_y)$ superconductivity-induced shift has to be compared with the initially small value of the mass of the charge susceptibility at $\mathbf{Q}_y$. We therefore focus on the renormalization of the polarization operators right at $\mathbf{q} = \mathbf{Q}_y$. The calculations, which we describe in more detail below, show expected trends – superconductivity competes with CO, and once long-range superconducting order develops, it tends to delay the appearance of CO. This effect is very typical for competing orders and has been recently discussed in detail for Fe-pnictides[37]. Because $\chi^{-1}(\mathbf{Q}_y)$ increases, both longitudinal and transverse charge correlation lengths go down. The data[13] show the same trend.

A more subtle issue is the magnitude of superconductivity-induced shift. Near T_c (i.e., for relatively small Δ_{sc}), the shift originates from $\beta_{ij}|\Delta_{sc}|^2\Delta_{k_i}^Q(\Delta_{k_j}^Q)^*$ terms in the Free energy, where, we remind, Δ_k^Q is fluctuating CO field (not the condensate), and k_i is either $\pm k_0$ or $\pm k_\pi$. Since the superconducting pair has zero total momentum, it couples to fermions located only within one corner of the Brillouin zone; hence coupling terms for $\pm k_0$ and $\pm k_\pi$ can be considered separately. At the same time, superconductivity pairs fermions with opposite momenta, hence both $|\Delta_k^Q|^2$ and $\Delta_k^Q(\Delta_{-k}^Q)^*$ couple to $|\Delta_{sc}|^2$.

For definiteness, let's set, as before, $\mathbf{Q} = \mathbf{Q}_y$ and focus on the region where center of mass momentum of charge

order parameter is $\pm k_0$. The Free energy is

$$F = \chi^{-1}(Q_y)\left(|\Delta_{k_0}^{Q_y}|^2 + |\Delta_{-k_0}^{Q_y}|^2\right) + |\Delta_{sc}|^2\left[\beta_{11}\left(|\Delta_{k_0}^{Q_y}|^2 + |\Delta_{-k_0}^{Q_y}|^2\right) + \beta_{12}\left(\Delta_{k_0}^{Q_y}(\Delta_{-k_0}^{Q_y})^* + (\Delta_{k_0}^{Q_y})^*\Delta_{-k_0}^{Q_y}\right)\right] \quad (2)$$

(We neglected spatial fluctuations of CO and terms unrelated to our purposes.) This Free energy is easily diagonalized by introducing $\Delta_d = (\Delta_{k_0}^{Q_y} + \Delta_{-k_0}^{Q_y})/\sqrt{2}$ and $\Delta_c = (\Delta_{k_0}^{Q_y} - \Delta_{-k_0}^{Q_y})/\sqrt{2}$. In terms of these variables

$$F = |\Delta_d|^2\left[\chi^{-1}(Q_y) + 2|\Delta_{sc}|^2(\beta_{11}+\beta_{12})\right] + |\Delta_c|^2\left[\chi^{-1}(Q_y) + 2|\Delta_{sc}|^2(\beta_{11}-\beta_{12})\right]. \quad (3)$$

We see that the shift of $\chi^{-1}(Q_y)$ due to superconductivity is generally different for symmetric density and antisymmetric current components of CO (Δ_d and Δ_c, respectively).

The couplings β_{11} and β_{12} can be evaluated either by using Hubbard-Stratonovich (HS) formalism, or by expanding particle-hole bubbles to order Δ_{sc}^2. In the HS formalism, these two terms are given by square diagrams made out of four fermionic Green's functions in the normal state (shown in Fig. 2c). We computed β_{11} and β_{12} for a model with hard cutoff and found that the dominant piece in each is a cutoff-independent term, which scales as $1/T$. At the lowest T, the expansion in powers of Δ_{sc} does not hold, and $1/T$ divergence is cut by $1/|\Delta_{sc}|$. Upon a more careful look, we found that universal (i.e., cutoff-independent) $1/T$ terms in β_{11} and β_{12} come with exactly opposite coefficients, i.e., $1/T$ terms cancel out in $\beta_{11}+\beta_{22}$. This cancellation has not been noticed before.[38] The subleading terms do not cancel. These subleading terms are, however, much smaller, and the correction to $\chi^{-1}(Q_y)$ from the superconducting order is given by $\alpha|\Delta_{sc}|^2/\Lambda \times \log(\Lambda/T)$ ($\alpha > 0$). The outcome is that the mass of the density component of charge order parameter (the one measured by x-ray) goes up in the presence of superconductivity (and the correlation length, which scales as inverse mass, goes down); however this effect is small. This small coupling between the competing charge density and superconducting orders also implies that the order which appears first does not rapidly destroy the other one, hence CDW and superconductivity co-exist over a sizable range of dopings.

At the same time, for the current CO component Δ_c^Q, Δ_{sc}^2/T contributions in β_{11} and β_{12} add up, i.e., for this component superconductivity has stronger negative impact. In particular, when CO emerges inside the superconducting dome, only its density component becomes non-zero when $-\chi^{-1}(Q) = |\Delta_{sc}|^2(\beta_{11}+\beta_{22}) \sim |\Delta_{sc}|^2/\Lambda$. Current component emerges at smaller dopings, when (and if) the condition $-\chi^{-1}(Q) = |\Delta_{sc}|^2(\beta_{11}-\beta_{22}) \sim |\Delta_{sc}|^2/(\max(T, |\Delta_{sc}|))$ is satisfied, and co-exists with superconductivity in a narrower range. We show this in Fig. 3. Since the current component of CO is responsible for the breaking of time-reversal symmetry (TRS),

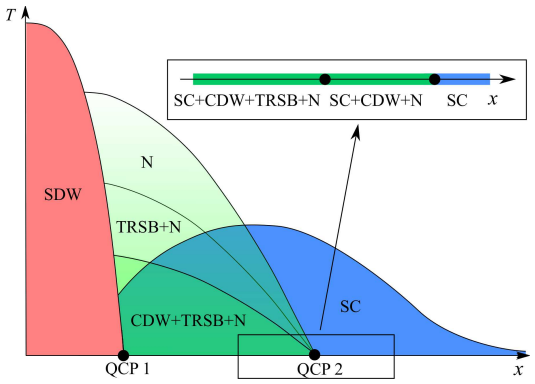

FIG. 3. The phase diagram in variables T and x (adapted from Ref. 18), with more details near $T = 0$ based on our new results (the inset). N and TRSB stand for nematic and time-reversal symmetry breaking in the pseudogap state, respectively, and CDW is the phase with broken translational symmetry (in a clean system).

its absence over some doping range where the density component of CO is present implies that in this range CO cannot be the source of TRS breaking. Alternatively speaking, if TRS breaking is caused by charge order, the end point of TRS breaking transition should end up at $T = 0$ at a smaller doping than the onset of CO. It would be interesting to test this in Kerr and elastic neutron scattering measurements in the superconducting state[39–41].

Summary.- In this paper we considered three aspects associated with uni-axial charge order in the underdoped cuprates. First, we analyzed the anisotropy of the charge order correlation length in the normal state, detected in recent x-ray measurements. Our goal was to investigate whether these data allow one to distinguish between magnetic and phonon-based mechanisms of CO formation. We argued that the magnetic scenario yields results consistent with the data in Ref. 13. Second, we argued that both longitudinal and transverse charge correlation lengths decrease in the presence of a true superconducting order, primarily because this order increases the mass of the charge order propagator. Finally, we found that the mass increase is different for the density and the current components of CO (symmetric and antisymmetric components with respect to the flip of a center of mass momenta of fermions which form CO). The mass increase is strong for the current component and is parametrically weaker for the density component. As a result, under the umbrella of superconductivity, the density component of CO exists in a wider range of doping compared to the current component. Since the current component of CO is responsible for TRS breaking, we propose to use this fact to test whether TRS breaking is associated with incommensurate charge order.

Acknowledgments.- We thank E. Berg, R. Fernandes and S. Sachdev for fruitful discussions. The work was supported by the NSF- DMR-1523036 (YW and AC) and DMR-1360789 (DC). YW has been also supported

by the Gordon and Betty Moore FoundationŠs EPiQS Initiative through Grant GBMF4305 at the University of Illinois. DC acknowledges the hospitality of FTPI, Minneapolis and PITP, Waterloo, where a part of this work was completed. AC and DC acknowledge hospitality of MPI-PKS, Dresden.

[1] J. Tranquada, B. Sternlieb, J. Axe, Y. Nakamura, and S. Uchida, Nature **375**, 561 (1995).
[2] J. Tranquada, J. Axe, N. Ichikawa, A. Moodenbaugh, Y. Nakamura, S. Uchida, Phys. Rev. Lett. **78**, 338 (1997).
[3] G. Ghiringhelli, M. Le Tacon, M. Minola, S. Blanco-Canosa, C. Mazzoli, N.B. Brookes, G.M. De Luca, A. Frano, D. G. Hawthorn, F. He, T. Loew, M. Moretti Sala, D.C. Peets, M. Salluzzo, E. Schierle, R. Sutarto, G. A. Sawatzky, E. Weschke, B. Keimer, and L. Braicovich, Science, **337**, 821 (2012).
[4] J. Chang, E. Blackburn, A. T. Holmes, N. B. Christensen, J. Larsen, J. Mesot, Ruixing Liang, D. A. Bonn, W. N. Hardy, A. Watenphul, M. v. Zimmermann, E. M. Forgan, and S. M. Hayden, Nat. Phys. **8**, 871 (2012).
[5] A. J. Achkar, R. Sutarto, X. Mao, F. He, A. Frano, S. Blanco-Canosa, M. Le Tacon, G. Ghiringhelli, L. Braicovich, M. Minola, M. Moretti Sala, C. Mazzoli, Ruixing Liang, D. A. Bonn, W. N. Hardy, B. Keimer, G. A. Sawatzky, and D. G. Hawthorn, Phys. Rev. Lett., **109**, 167001 (2012).
[6] R. Comin, A. Frano, M. M. Yee, Y. Yoshida, H. Eisaki, E. Schierle, E. Weschke, R. Sutarto, F. He, A. Soumyanarayanan, Y. He, M. Le Tacon, I. S. Elfimov, J. E. Hoffman, G. A. Sawatzky, B. Keimer, and A. Damascelli, Science **343**, 390 (2014)
[7] E. H. da Silva Neto, P. Aynajian, A. Frano, R. Comin, E. Schierle, E. Weschke, A. Gyenis, J. Wen, J. Schneeloch, Z. Xu, S. Ono, G. Gu, M. Le Tacon, A. Yazdani, Science **343**, 393 (2014).
[8] K. Fujita, M. H. Hamidian, S. D. Edkins, C. K. Kim, Y. Kohsaka, M. Azuma, M. Takano, H. Takagi, H. Eisaki, S. Uchida, A. Allais, M. J. Lawler, E.-A. Kim, S. Sachdev, and J. C. Séamus Davis, Proc. Nat. Acad. Sci, **111**, E3026 (2014).
[9] Tao Wu, Hadrien Mayaffre, Steffen Krämer, Mladen Horvatić, Claude Berthier, W. N. Hardy, Ruixing Liang, D. A. Bonn, and Marc-Henri Julien, Nature **477**, 191-194 (2011); T. Wu, H. Mayaffre, S. Krämer, M. Horvatić, C. Berthier, W.N. Hardy, R. Liang, D.A. Bonn, and M.-H Julien, Nat. Comm. **6**, 6438 (2015).
[10] S. A. Kivelson, E. Fradkin, and V. J. Emery, Nature **393** 550 (1998).
[11] S. A. Kivelson, I. P. Bindloss, E. Fradkin, V. Oganesyan, J. M. Tranquada, A. Kapitulnik, and C. Howard, Rev. Mod. Phys. **75**, 1201 (2003).
[12] M. H. Hamidian, S. D. Edkins, Chung Koo Kim, J. C. Davis, A. P. Mackenzie, H. Eisaki, S. Uchida, M. J. Lawler, E.-A. Kim, S. Sachdev, and K. Fujita, arXiv:1507.07865; M. H. Hamidian, S. D. Edkins, K. Fujita, A. Kostin, A. P. Mackenzie, H. Eisaki, S. Uchida, M. J. Lawler, E.-A. Kim, S. Sachdev, and J. C. Davis, arXiv:1508.00620
[13] R. Comin, R. Sutarto, E. H. da Silva Neto, L. Chauviere, R. Liang, W. N. Hardy, D. A. Bonn, F. He, G. A. Sawatzky, A. Damascelli, Science, **347** 1335 (2015).
[14] S. Blanco-Canosa, A. Frano, E. Schierle, J. Porras, T. Loew, M. Minola, M. Bluschke, E. Weschke, B. Keimer, and M. Le Tacon, Phys. Rev. B **90**, 054513 (2014).
[15] M. A. Metlitski and S. Sachdev, Phys. Rev. B **82**, 075128 (2010).
[16] K. B. Efetov, H. Meier and C. Pepin, Nat. Phys. **9** 442 (2013); H. Meier, M. Einenkel, C. Pépin, K. B. Efetov, Phys. Rev. B **88**, 020506 (2013); H. Meier, C. Pepin, M. Einenkel and K.B. Efetov, Phys. Rev. B **89**, 195115 (2014); K. B. Efetov Phys. Rev. B 91, 045110 (2015).
[17] S. Sachdev and R. La Placa, Phys. Rev. Lett. **111** 027202 (2013); A. Allais, J. Bauer and S. Sachdev, Phys. Rev. B **90** 155114 (2014).
[18] Y. Wang and A. V. Chubukov, Phys. Rev. B **90** 035149 (2014). See also A. Tsvelik and A. V. Chubukov, Phys. Rev. B **89**, 184515 (2014).
[19] P. A. Lee, Phys. Rev. X **4**, 031017 (2014).
[20] C. Pépin, V. S. de Carvalho, T. Kloss, X. Montiel, Phys. Rev. B **90**, 195207 (2014); H. Freire, V. S. de Carvalho, and C. Pépin, arXiv:1503.00379 (2015); T. Kloss, X. Montiel, C. Pépin, arXiv:1501.05324 (2015).
[21] D. Chowdhury and S. Sachdev, Phys. Rev. B **90**, 134516 (2014).
[22] D. Chowdhury and S. Sachdev, Phys. Rev. B **90**, 245136 (2014).
[23] E. Fradkin, S. A. Kivelson, J. M. Tranquada, arXiv:1407.4480.
[24] S. Bulut, W. A. Atkinson, and A. P. Kampf, Phys. Rev. B **88**, 155132 (2013); W. Atkinson, A. Kampf and S. Bulut, New J. Phys. **17** 013025 (2015); W. A. Atkinson and A. P. Kampf, Phys. Rev. B **91**, 104509 (2015).
[25] D.F. Agterberg, D.S. Melchert, and M.K. Kashyap, Phys. Rev. B **91**, 054502 (2015).
[26] Y. Wang, D. Agterberg, and A. V. Chubukov, Phys. Rev. B **91**, 115103 (2015); Phys. Rev. Lett. 114, 197001 (2015).
[27] Y. Wang and A.V. Chubukov, Phys. Rev. B **91**, 195113 (2015).
[28] C. Castellani, C. Di Castro, and M. Grilli, Phys. Rev. Lett. **75**, 4650 (1995); A. Perali, C. Castellani, C. Di Castro, and M. Grilli, Phys. Rev. B **54**, 16216 (1996); C. Castellani e al., J. Phys. Chem. Sol. **59**, 1694 (1998); A. Perali *el al*, Phys. Rev. B **62**, R9295(R) (2000); S. Andergassen, S. Caprara, C. Di Castro, and M. Grilli, Phys. Rev. Lett. 87, 056401 (2001); G. Seibold et al, Physica C **481**, 132 (2012).
[29] A. Georges, G. Kotliar, W. Krauth, and M. J. Rozenberg Rev. Mod. Phys. **68**, 13 (1996); P. A. Lee, N. Nagaosa, and X-G Wen, Rev. Mod. Phys. **78**, 17 (2006); D. B. Kyung, S. S. Kancharla, D. Sénéchal, A.-M. S. Tremblay, M. Civelli, and G. Kotliar, Phys. Rev. B **73**, 165114 (2006); E. Gull, O. Parcollet, and A. J. Millis, Phys. Rev. Lett. **110**, 216405 (2013); G. Sordi, P. Sémon, K. Haule, and A.-M. S. Tremblay Phys. Rev. B **87**, 041101(R) (2013); Ara Go and A. J. Millis, Phys. Rev. Lett. **114**, 016402 (2015) and references therein
[30] It is important to note here that the CDW peaks reported in energy-integrated x-ray measurements[13] are still primarily determined by the elastic processes and therefore reflect the underlying static CO. Hence we shall only be interested

in the static susceptibility evaluated at $\omega = 0$.

[31] J. A. Robertson, S. A. Kivelson, E. Fradkin, A. C. Fang, and A. Kapitulnik, Phys. Rev. B **74**, 134507 (2006); A. Del Maestro, B. Rosenow, and S. Sachdev, Phys. Rev. B **74**, 024520 (2006), and references therein.

[32] Y. Wang and A. V. Chubukov, arXiv:1507.03583.

[33] Y. Wang, A. V. Chubukov, and R. Nandkishore, Phys. Rev. B 90, 205130 (2014); M. Gradhand, I. Eremin, and J. Knolle, Phys. Rev. B **91**, 060512(R) (2015).

[34] L. Nie, G. Tarjus, and S. A. Kivelson, Proc. Nat. Acad. Sci. **111**, 7980 (2014); L. Nie, L. E. H. Sierens, R. G. Melko, S. Sachdev, and S. A. Kivelson, arXiv:1505.06206.

[35] V. Mishra and M. R. Norman, arXiv:1502.02782 (2015).

[36] See Supplemental Material at [URL will be inserted by publisher] for computation of the polarization bubble.

[37] R. Fernandes and J. Schmalian, Phys. Rev. B 82, 014521 (2010); A.B.Vorontsov, M.G.Vavilov, and A.V.Chubukov, Phys. Rev. B 81, 174538 (2010).

[38] From a mathematical perspective, this cancellation is similar to the cancellation between vertex and self-energy corrections to uniform density-density correlator. In the latter case, however, the cancellation is exact and it enforces Ward identity associated with particle number conservation. In our case, the cancellation is not required by symmetry and is not exact – only the leading $1/T$ terms cancel out in $\beta_{11} + \beta_{12}$.

[39] J. Xia, E. Schemm, G. Deutscher, S. A. Kivelson, D. A. Bonn, W. N. Hardy, R. Liang, W. Siemons, G. Koster, M. M. Fejer, and A. Kapitulnik Phys. Rev. Lett. **100**, 127002 (2008); H. Karapetyan, J. Xia, M. Hucker, G. D. Gu, J. M. Tranquada, M. M. Fejer, and A. Kapitulnik, Phys. Rev. Lett. **112**, 047003 (2014). See also Y. Lubashevsky, LiDong Pan, T. Kirzhner, G. Koren, and N. P. Armitage, Phys. Rev. Lett. **112**, 147001, (2014).

[40] W. Tabis, Y. Li, M. Le Tacon, L Braicovich, A. Kreyssig, M. Minola, G. Dellea, E. Weschke, M. J. Veit, M. Ramazanoglu, A. I. Goldman, T. Schmitt, G. Ghiringhelli, N. BariŽic, M. K. Chan, C. J. Dorow, G. Yu, X. Zhao, B. Keimer, and M. Greven, Nature Communications 5, 5875 (2014).

[41] L. Mangin-Thro, Y. Sidis, A. Wildes, P. Bourges, Nat. Comm. **6**, 7705, (2015) and references therein.